

Atomic clusters, local isomorphism, and recurrently localized states in quasicrystals

This article has been downloaded from IOPscience. Please scroll down to see the full text article.

1997 J. Phys.: Condens. Matter 9 1493

(<http://iopscience.iop.org/0953-8984/9/7/013>)

View [the table of contents for this issue](#), or go to the [journal homepage](#) for more

Download details:

IP Address: 171.66.16.207

The article was downloaded on 14/05/2010 at 08:07

Please note that [terms and conditions apply](#).

Atomic clusters, local isomorphism, and recurrently localized states in quasicrystals

C Janot

Institut Laue–Langevin, BP 156, 38042 Grenoble Cédex 9, France

Received 28 August 1996

Abstract. Perfect icosahedral quasicrystals have a structural skeleton based on hierarchical selfsimilar packing of atomic clusters. The related inflation rules constrain both composition and atomic valences to have strictly defined values. Stability of the skeleton requires that bonding electrons are recurrently localized at sites forming selfsimilar isomorphic subsets of the structure and are distributed into ‘magic’ cluster states. The corresponding eigenstates show power law dependences in space which generate a hopping mechanism for conductivity and unexpected physical properties.

1. Introduction

Quasicrystals (QCs) are a new form of the solid state which differs from the other two known forms, crystalline and amorphous, by possessing a new type of long-range translational order, *quasiperiodicity*, and a noncrystallographic orientational order [1–3]. A central problem in condensed-matter physics is to determine whether quasiperiodicity leads to new physical properties which are significantly different from those of crystalline and amorphous materials. Such unusual properties have been found in icosahedral (i) alloys of high structural quality [4–7]. Some of their most striking features, which are not expected for alloys consisting of normal metallic elements, are the very high value of the electrical resistivity (up to $\sim 10 \Omega \text{ cm}$ at low temperatures in the i-Al-Pd-Re system [8–11]), a strong negative temperature coefficient of resistivity, an increase of resistivity with increased structural perfection of the samples along with an extreme sensitivity to sample composition, and a low, if any, electronic contribution to the specific heat and thus a vanishing density of states (DOS) at the Fermi level.

Other peculiar properties of QCs include thermal insulator behaviour, difficult wetting of the surface, low friction coefficient, high hardness, elevated corrosion resistance, and a brittle–ductile transition with very soft plasticity above about 700°C [7, 12, 13]. Most of these properties combine effectively to give technologically interesting applications [14].

Differences between periodic crystals (PCs) and QCs show up in either real or reciprocal space. Both viewpoints are useful for understanding some of the properties of QCs. The starting ingredient to generate both PCs and QCs is a finite set of atomic units of finite sizes which defines local symmetries (point group) and chemical order of the structure to be grown. Then, PCs can be obtained via addition rules which define the Bravais lattice with its translational invariance. To obtain QCs, substitution rules must be used instead, in such a way that the result is a perfectly ordered, deterministic arrangement of atoms, without any indication of periodicity. Substitution operations, although far less simple than translation

algorithms, are the only way to grow an ordered structure with atomic units having both high bonding energies and ‘forbidden’ symmetries (e.g. icosahedral morphology).

In a monatomic PC such as a metal crystal, all atomic sites are strictly equivalent. If some electrons are loosely bonded to atoms, they have no reason to locate on a particular site and can travel essentially freely through the bulk of the metal. The result is high conductivity, isotropy of the properties, strain–stress characteristics, and well known consequences for practical behaviours and applications. Conversely, strictly equivalent sites cannot be found in QC structures. The ‘free’ valence electrons, if there are any, are actually forced to ‘locate’ preferably at low-energy sites within the constraints of the Coulomb interaction.

This statement must actually be somewhat smoothed out. QC structures are locally isomorphic, which means that identical atomic clusters of any size can be found at distances apart of about twice their size. These identical clusters form selfsimilar subsets of the structure over which electronic and vibrational states are expected to extend, with hopping or/and tunnelling communication between sites of a given subset.

The reciprocal space description of QCs adds to our understanding and supports similar conclusions. Both PC and QC structures can be analysed in terms of their Fourier components: the space dependence of their density is indeed easily expressed as a sum of density waves. For PCs, the corresponding wave vectors \mathbf{G} define a discrete reciprocal lattice and each \mathbf{G} vector is an integer linear combination of three basis vectors related to the translation of the Bravais lattice. For QCs, the number of integer linearly independent vectors required to span the reciprocal space exceeds the space dimension (e.g. six basis vectors for icosahedral structures) and the \mathbf{G} vectors fill the space densely. Inferred differences between PCs and QCs include the analysis of wave propagation. Plane waves with any wave vector \mathbf{k} propagate easily through periodic structures except for those rare \mathbf{k} vectors which satisfy the Bragg law and, then, are diffracted. These exceptions generate two-component standing waves; they remain extended but do not contribute to propagation or to energy transport. In QCs, the exception becomes the rule since the \mathbf{G} vectors form a dense set. Thus, any \mathbf{k} vector can comply with diffraction conditions. Moreover, as it can be easily inferred from a simple geometrical derivation based on the Ewald sphere, multiple diffraction occurs generally and the number of individual plane waves contributing to the resulting steady state increases with $|\mathbf{k}|$. However, many contributions $F(\mathbf{G})$ of the structure factor are very small in QCs, which damps down the diffraction effects for the \mathbf{k} states involving the corresponding \mathbf{G} vectors and macroscopic mean free path cannot be excluded completely. Another consequence of the set of \mathbf{G} vectors being dense in QCs is that momentum of vibrational excitations can be transferred to the quasilattice in inelastic scattering events by small quantities not limited from below in magnitude; this transfer increases with $|\mathbf{k}|$ because of the possibility for the \mathbf{k} state to couple with a larger subset of \mathbf{G} components of the structure if $|\mathbf{k}|$ is large. In other words an ‘umklapp’-like process is rather the rule than the exception in QCs. Thus, everything seems to contribute to make propagation phenomena difficult in QCs even though some sort of recurrent localized states may allow transport effects.

Calculations of eigenstates for propagation of electrons or atomic vibration in QCs have been extensively produced [15–20]. All these approaches are based on substitution of periodic approximant structures to QCs, in order to be able to use calculation methods currently applied to PCs. The results are useful and very often appear as consistent with experimental data, within accuracy and resolution limits of course, but this may be as blind an alley as the attempted analyses of the QC structure proposed by Pauling some ten years ago, with the great risk of passing away from new concepts.

A more interesting approach has been initiated recently, with the analysis of the influence of an atomic cluster when embedded in a 'free-electron' metallic matrix [21, 22]. This has led to the notion of 'cluster virtual bound states' corresponding to resonances of the free-electron wave functions with cluster levels at different length scales.

In this paper, we are going to take advantage of a full analysis of QC structure in terms of selfsimilar subsets of isomorphic domains to go a little further and to describe eigenstates as recurrently localized, which is an attempt to combine multiple location in space with relatively poor transport properties.

2. Why should quasicrystals form?

While there has been significant progress in the understanding of the growth of quasiperiodic order [23], the basic issue of the energetics of growth has remained largely unexplained. However, a consensus seems to emerge progressively that quasiperiodic long-range order is somewhat forced by the trend of atoms to gather into very stable clusters having noncrystallographic symmetries. The latter is obviously a requisite to prevent periodic growth and the former is necessary if the clusters have to keep their morphological identity when assembled to form bigger units. This idea that local rules may be responsible for long-range order has been recently supported by numerical simulations [24]. A model which presupposes the existence of two kinds of cluster and uses energetic considerations for the growth of chemically long-range ordered compounds has been proposed by Quémenerais [25]. The model shows that the electronic structure of the clusters can drive the system towards quasiperiodic growth. One assumes that there are two kinds of cluster, A and B. Let v_A and v_B be the valence and e_A and e_B the one-electron energy levels respectively. Different growth patterns emerge depending on the values of e_A , v_A , e_B , and v_B . In particular, for specific nonintegral values of v_A and v_B , a simple tight-binding calculation of the energy shows that the quasiperiodic arrangement is preferred. Molecular dynamics calculations by Dzugutov [26] have also demonstrated that a particle assembly, when allowed to relax into a locally strong icosahedral potential, reaches long-distance quasiperiodic order.

Last but not least, such atomic clusters have been experimentally observed in the structure of real QCs. Indeed, building units of about 50 atoms with geometry close to that of a Mackay icosahedron have been identified in AlPdMn and AlFeCu QCs either in their structures as deduced from diffraction data [2, 3, 27–29] or directly with imaging techniques such as secondary-electron imaging [30], x-ray photoelectron diffraction [31], or scanning tunnelling microscopy [32].

Conditions for stability of atomic clusters can be understood from the developing subject of the physics of free atomic clusters. Free clusters are almost always generated and studied in molecular beams. When assembled, most clusters coalesce to form bigger units and the properties evolve to the bulk. This confirms that, if the clusters are to serve as building blocks, they have to be such that they will not lose their identity when assembled. This can be accomplished if the clusters are very stable and resist deformation. That this is possible is already evident from the discovery of fullerenes, which are crystals of C_{60} clusters. Another cluster with the potential of forming cluster assemblies was discovered by Guo *et al* [33]. It is made up of eight transition metal and 12 carbon atoms and is referred to as a metallo-carbohedrene. Both these are experimental discoveries. Is it possible to develop some fundamental principles which could guide us to identify clusters with potential for forming cluster materials?

To gain an insight into the above question, it is helpful to look at the factors controlling the stability and reactivity of clusters. Let us start with the abundance spectra of Na_n clusters

generated in beams [34]. They show that the clusters containing two, eight, 18, 20, 40, 58, 92, ... Na atoms are far more dominant than other sizes. These special clusters are said to contain the magic numbers of atoms. Theoretical work shows that this can be understood on the basis of a simple jellium model where one imagines that the positive charges of the ions are distributed over the size of the cluster and the electrons move in this effective potential. This is similar to the case of atoms except that in an atom the positive charge is localized at the nucleus. The one-electron levels in the jellium picture can be labelled using the same quantum numbers as in atoms because of the spherical symmetry of the potential. This is shown in figure 1. In a cluster, the level order is $1s^2 1p^6 1d^{10} 2s^2 1f^{14} 2p^6 1g^{18} \dots$. It is easy to see that the magic clusters two, eight, 20, 34, 40, 58, 92, ... correspond to clusters with filled shells, i.e. $1s^2, 1s^2 1p^6, 1s^2 1p^6 1d^{10} 2s^2, \dots$. The filled electronic shells should also make these clusters behave like inert gas atoms. In fact they do. For example, the ionization potential on Na_n clusters shows peaks at clusters containing two and eight electrons (atoms) as in the case of atoms where the maxima occur at inert gases with two or eight electrons. The magic clusters are also chemically less reactive. For example, experimental studies of the reactivity of Al_n [35] with oxygen show that, whereas Al_{13} reacts strongly, $(Al_{13})^-$ with 40 electrons and a filled electronic shell is relatively inert. These results show that the electronic structures of clusters resemble those of atoms and the most stable clusters correspond to filled electronic shells, which also render them less reactive.

It was Khanna and Jena [36–38] who first argued that it should be possible to design very stable clusters mimicking different elements in the periodic table. They considered an Al_{13} cluster. The ground state is an icosahedron having a central atom surrounded by a first shell of 12 atoms. The cluster is geometrically close packed. Al is trivalent, so the cluster has 39 bonding electrons, one shy of the magic number 40. The cluster could therefore be made more stable by doping with a tetravalent impurity such as C. Using *ab initio* calculations, they showed that an $Al_{12}C$ cluster is indeed more stable than Al_{13} by 4.4 eV. The electronic shell filling also makes the cluster less reactive. A calculation of the binding energy of a H atom brought towards Al_{13} and $Al_{12}C$ showed that the binding energy is significantly reduced in the case of $Al_{12}C$. The final test to the stability and inertness has come from the recent computer simulations of a molecule composed of two $Al_{12}C$ units. The studies based on Car–Parinello quantum molecular dynamics show that the structure of the individual $Al_{12}C$ clusters remains intact. We would like to add that a similar study on $Al_{12}Si$ which also has 40 electrons showed that the energy gain is smaller. The energy gain in $Al_{12}C$ is due to the electronic shell filling as well as due to the fact that C is smaller than Al and therefore allows the surface Al–Al bonds, which are 5% longer than radial bonds in an ideal icosahedron, to relax.

In the above, we have discussed designing relatively inert clusters. One can also form assemblies using molecular units composed of clusters interacting via ionic or covalent bonds. Consider the Al_{13} cluster. In a jellium model, its electronic state corresponds to $1s^2 1p^6 1d^{10} 2s^2 1f^{14} 2p^5$. It therefore requires one more electron to fill the p shell just as a halogen atom. A theoretical calculation shows that it indeed has an electron affinity of 3.7 eV compared to 3.6 eV for the Cl atom. Note that an Al atom has an electron affinity of only 0.6 eV. A theoretical calculation for the KAl_{13} cluster shows that the K loses its electron to Al_{13} and the molecule has a binding energy of 3.04 eV due to the formation of an ionic bond.

The above discussion shows that, by controlling the number of atoms and the chemical composition, it is possible to have clusters which can mimic different atoms in the periodic arrangement. These clusters can serve as building blocks in much the same way as atoms.

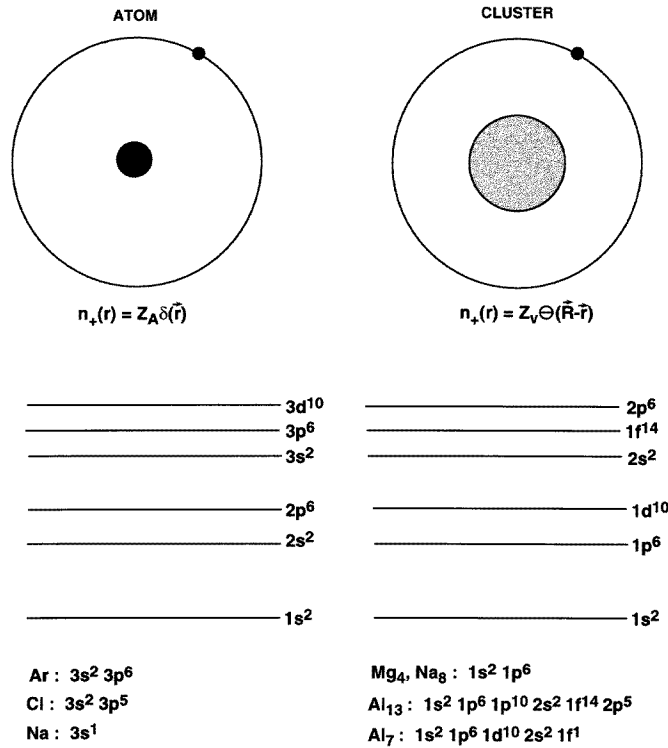


Figure 1. Comparison of the one-electron energy levels in an atom and a cluster (superatom). Examples of clusters simulating different atoms are also given.

Figure 2 shows the one-electron levels (only the valence portion) of an Al atom and an Al₁₃ cluster. In an atom, the degeneracy of the one electron levels is governed by the angular momentum quantum number. In a cluster, on the other hand, the degeneracy is governed by the arrangement of atoms. Whereas an atom only undergoes a change in electronic orbital upon chemical bonding, a cluster is a soft superatom where the atomic structure can also change. The resistance to such a change depends on the binding energy of the cluster, the energy cost for deformation and the binding energy between clusters.

In this context, growth of icosahedral QCs may result from a special situation regarding the number of valence electrons available in the basic cluster as compared to a close magic number [27–29]. Consider a cluster made of N atoms, taken as all identical for simplicity, with n valence (or bonding) electrons per atom such that the total number of electrons Nn differs from a magic number M by n :

$$Nn = M + n$$

or

$$n = M/(N - 1). \tag{1}$$

Since it misses the magic number M , the cluster would be slightly reactive and it will have a tendency to assemble with $N - 1$ identical clusters to grow into a supercluster (of N clusters) containing again $Nn = M + n$ bonding electrons, missing again the ‘magic stability’ to allow further growth into inflated selfsimilar supersuperclusters and so on and

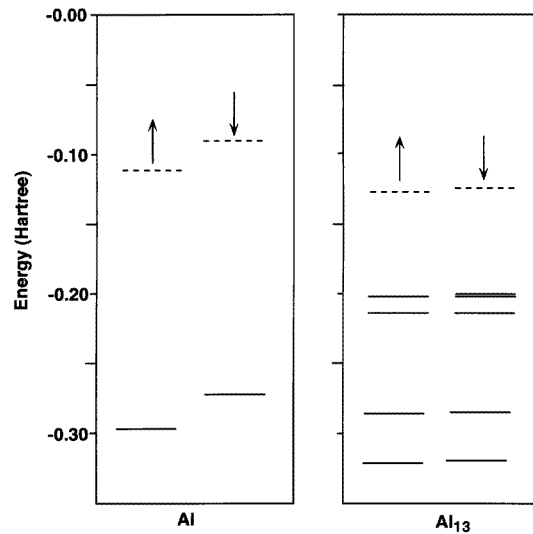


Figure 2. (a) Energy levels in an Al atom. (b) Energy levels of electrons in an Al₁₃ cluster.

so forth. From a physical point of view, the picture assumes the cluster behaves as a square well confining most of the electrons. Only electrons close to the Fermi energy tunnel through the barrier but most of the new states are confined by the well created by the succeeding supercluster and so on. The electron density of states $n(E)$ is thus composed of the unlocalized states of one generation falling on to the localized states of the next generation. It is schematically shown in figure 3. The width of the successive sub-bands decreases rapidly, following the squared sizes of the successively inflated domains. The density of states at low energy is mastered by the basic 'small' cluster and is terminated toward the Fermi level by a succession of selfsimilar, more and more spiky features. The overall envelope of the spikes follow a power law of energy $E^{1/2}$ in good agreement with experimental results [39]. Such a model has observable implications including poor conductivity (increasing with temperature), low chemical reactivity, diamagnetism, and mechanical brittleness.

To go beyond the model toward real QCs, there are two difficulties which are not easily overcome: real QCs are never monatomic systems (they belong mostly to ternary systems), it seems that their structures cannot be covered with a single type of cluster, and selfsimilar packing does not necessarily have the expected density. These drawbacks of the model will be illustrated and partially overcome in the next section with the example of the AlPdMn QC.

Obviously, saying that the structure of QCs can be described by selfsimilar packing of building blocks is not a discovery: everybody has realised that for a very long time. What is somewhat new and may be useful in the above derivation includes:

(i) the idea that the structure is robustly quasiperiodic if the building blocks are 'almost magic' clusters with noncrystallographic symmetries and

(ii) the consequence that most of valence electrons of the atoms are 'virtually' trapped in cluster-like levels within a selfsimilar jellium following the constraints of the structure. The result is a sort of multiple-site selfsimilar localization. This has not to be taken too strictly: the atomic clusters are not isolated from each other; electrons may jump continuously from

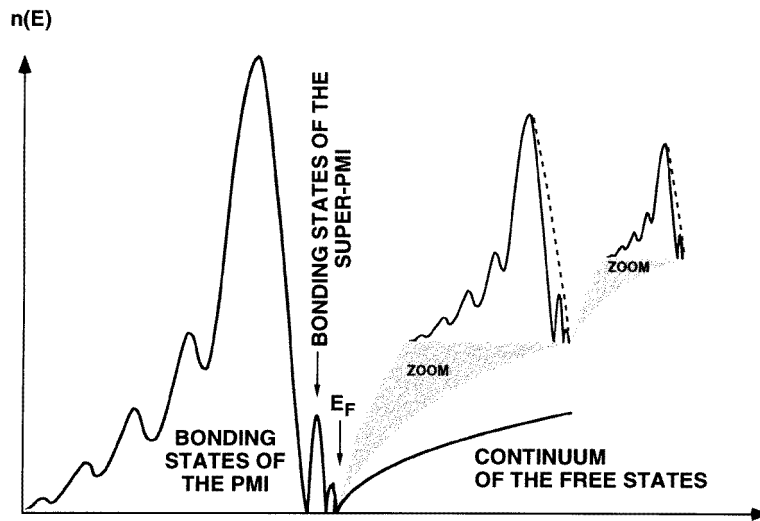


Figure 3. Schematic density of electronic states for AlPdMn QCs. The large feature on the left-hand side is the contribution of the elementary PMI. The successive features arise from the inflated PMIs.

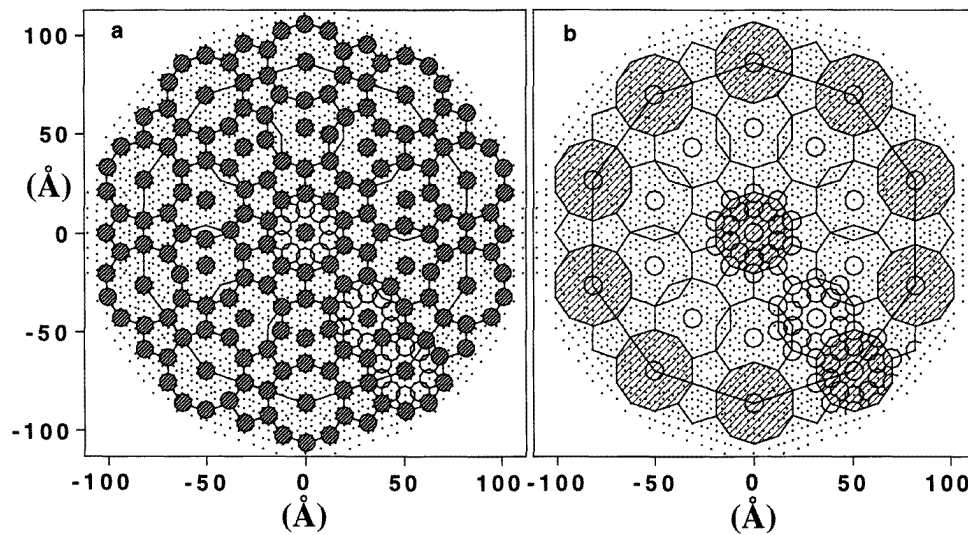


Figure 4. A piece of a planar cut perpendicular to a fivefold axis of one possible configuration of the structure of an AlPdMn quasicrystal. Hatched patches mark subsets of locally isomorphic domains. (a) The state of the basic unit; (b) the state of the one time inflated domains.

site to site provided that the numbers of electrons in clusters of any scale remain magic when averaged in time [21,22]. This should also prevent any appearance of collective modes such as plasmon oscillations; the point has indeed been confirmed experimentally [40].

3. Almost magic clusters and selfsimilarity constraints in AlPdMn quasicrystals

Details of preparation and characterization of AlPdMn QCs, including those in the form of perfect large centimetre size single grains, have been published elsewhere [3, 4, 41–44]. Techniques relevant to quasicrystallography have also been extensively and critically presented on several occasions [1–3]. Though known at a rather low-level resolution only, the observed structure reveals several building rules which appear astonishingly simple, with both chemical and geometrical order.

First of all, the observed structure is essentially based on atomic units containing 51 atoms in total, named pseudo-Mackay icosahedra (PMIs) hereafter, and made of three centrosymmetrical shells: an inner small centred core of nine atoms, an intermediate icosahedron of 12 atoms and an external icosidodecahedron of 30 atoms. The last two shells have practically equal radii and constitute altogether the ‘surface’ of the PMI, whose diameter is very close to 9.6 Å. The small inner core is a piece of a pentagonal dodecahedron whose 20 atomic sites are only partially occupied in a way which probably fluctuate from PMI to PMI. Two families of chemically differing PMIs have been identified in the structure: one family (PMI-A) has something close to six manganese and six palladium atoms on the icosahedron sites of the external shell, the 39 remaining sites being occupied by aluminium atoms; the second family (PMI-T) has about 20 palladium atoms among the 42 sites of the external shell, the 31 or so remaining sites being occupied by aluminium atoms. The calculated atomic density of an individual PMI is 0.064 atoms Å⁻³, which is close to the measured density of the bulk material, within experimental accuracy. Chemical compositions of PMI-A and PMI-T as reported above cannot be strictly ascertained from diffraction data. We have shown elsewhere [28, 29] however that these PMI compositions are selfconsistently related to the combined constraints of the alloy composition and the selfsimilarity rules of the structures. Treating the AlPdMn QC as a pseudo-binary system, we have been also able to demonstrate that the pertinent magic number is here equal to 92 [28, 29, 45] and that the transition-metal atoms behave as if they had negative valences, v_{Pd} being only slightly negative and v_{Mn} being close to -3 . Such negative valences for transition-metal atoms have been recently suggested in intermetallic compounds; they are well consistent with the analysis of Mayou *et al* [21, 22] in terms of cluster virtual bound states and they suggest the trend of the d elements in these alloys to saturate their electron d levels by attracting electrons from Al atoms; the point has indeed received experimental support [46, 47]. Even the values $v_{Pd} \sim -0$ and $v_{Mn} \sim -3$ can be qualitatively understood. The electronic structures of Pd and Mn free atoms are 4d⁸ 5s² and 3d⁵ 4s² respectively; nearest-neighbour distances in QCs have been found to be up to more than 5% shorter than in the corresponding metals which generate large local pressure on electronic states; this has been experimentally shown to force transfer of electrons from s to d states [48] with the consequence that electrone-like materials can be obtained where atoms become ions with ‘interstitial’ electrons only. Then the electronic structure of Pd and Mn in QCs should approach 4d¹⁰ and 3d⁷ respectively, with a trend for Mn atoms to attract three more electrons so as to reach the 3d¹⁰ configuration, from a time averaging point of view.

Finally, we have also previously explained that the selfsimilar growth of the structure, or at least its skeleton, can proceed via successive substitutions of atoms by PMI with proper rescaling [28, 29, 45]. However, it would be dangerous to think that the reality is that simple. A minor remark regards density, which must be kept constant at any inflation stage; as substitution of atoms by PMIs increases the number of atoms by a factor of 51, the inflated volume must be also multiplied by 51 to avoid density losses; the scale factor

(defining length expansion) must then be $\sqrt[3]{51} = 3.7084\dots = (1.5478\dots)^3$, involving the number $\nu \approx 1.548$, which is very close to the observed value and falls only 4% off the golden mean τ used previously for simplicity [28, 29]. The detailed examination of the growth scheme reveals [28, 29] that some clusters overlap at any inflation stage.

A more basic remark concerns what we may call a requirement for intrinsic disorder even if the expression is not fully appropriate. The point is that the three-dimensional real structure of QCs is not univocally defined from diffraction data. The best to be expected is the six-dimensional periodic image of the three-dimensional quasiperiodic system which then results from slicing by the physical space. Many configurations, equally probable, are obtained when translating continuously this physical space in the hyperspace. The real structure may be a patchwork of domains each taken in one of the possible configurations, with interfaces or connecting regions in between implying phason defects. These defects are frozen in at low temperature but may generate atom jumps when the thermal energy is high enough, with softening of the material [49] and cleaning of weak diffuse scattering contributions from diffraction patterns [50].

Even so, selfsimilarity remains the most robust ingredient of the overall structure and this must be considered in its manifold aspects, i.e. not only via the already mentioned geometrical implications. For instance, valences must be extended from atoms to clusters at any inflation stage, with a one-to-one correspondence scheme. This means that, starting with three atomic species, i.e. Al, Pd and Mn, we must continue with three building units, i.e., PMI-Al, PMI-Pd and PMI-Mn. Two types of PMI only being deduced from diffraction data must then be accepted as an experiment-limited result with the PMI-T being the best observable compromise between PMI-Pd and PMI-Mn. Constraints from selfsimilarity requirements may allow us to discriminate between the two.

Let us first consider that some of the PMI-T are the inflated partners of the Pd atoms. The magic number invariance with inflation ($M = 92$ in the present case) imposes that the number of valence electrons in a PMI-Pd is $92 + v_{Pd}$ (v_{Pd} are the valences of the Pd atoms); if x_{Al} is the number of Al atoms over the 51 in the PMI, we have the trivial equation

$$3x_{Al} + (51 - x_{Al})v_{Pd} = 92 + v_{Pd} \quad (2)$$

in which v_{Pd} must be slightly negative, very close to zero indeed, and x_{Al} is an integer; v_{Pd} fixed to zero gives $x_{Al} = 30.66$, whose closest integers are 30 and 31. Using now $x_{Al} = 31$ (and $x_{Pd} = 20$ since PMI-T contains only Al and Pd atoms), one finds $v_{Pd} = -1/19 = -0.0526\dots$. With the other possible value $x_{Al} = 30$ ($x_{Pd} = 21$) and keeping $v_{Pd} = -1/19$, we have the second type of PMI-T, which happens to contain 88.8947... valence electrons, i.e. $92 - 3.1053$, whose 'cluster valence' is then -3.1053 ($3 + 2/19$ actually). This nicely sounds like PMI-Mn, the inflated partner of Mn atoms, with common valences equal to $-3.1053\dots$. Both PMI-Pd (31 Al + 20 Pd) and PMI-Mn (30 Al + 21 Pd) are fascinatingly close to the experimentally built PMI-T, well within practical resolution.

The other experimental family, PMI-A, can then be confidently assigned to Al atoms, with a +3 valence value ($92 + 3 = 95$ electrons in the PMI). Again the solution is very close to the experimental insight; with 38 Al atoms, six Mn atoms (half of the large icosahedron) and seven Pd atoms (the other half of the large icosahedron plus probably atoms at centres of the PMIs) we obtain the expected +3 valence. Thus, refining the experimental results in selfconsistency with inflation invariance of the structure and the magic cluster model allows us to approach more closely the real atomic clusters. A very pleasant by-product conclusion is that the three ingredients of the overall description (magic clusters, PMI units, and global inflation) can be considered as very robust.

To be completely conclusive on this point, we must also check selfconsistency of the model with the alloy composition which may be written as $\text{Al}_x\text{Pd}_y\text{Mn}_z$. After the first inflation stage we have the following situation:

$$\begin{aligned} x & \text{ PMI-Al which contain } 38 \text{ Al} + 7 \text{ Pd} + 6 \text{ Mn} \\ y & \text{ PMI-Pd which contain } 31 \text{ Al} + 20 \text{ Pd} \\ z & \text{ PMI-Mn which contain } 30 \text{ Al} + 21 \text{ Pd} \end{aligned} \quad (3)$$

with the resulting equations:

$$\begin{aligned} 51x &= 38x + 31y + 30z \\ 51y &= 7x + 20y + 21z \\ 51z &= 6x \end{aligned} \quad (4)$$

and the closing condition $x + y + z = 1$.

This over determined system of equations has actually one and only one solution i.e.

$$x = 0.702\,666\dots \quad y = 0.214\,666\dots \quad z = 0.082\,666\dots \quad (5)$$

which is impressively close to the composition of the AlPdMn icosahedral phase as shown in the experimentally built phase diagram [51]. It is noteworthy that the partial volume occupied by all Al atoms in the structure is close to being τ^2 times as large as the cumulated partial volumes of all Pd and all Mn atoms.

We may consider the demonstration as convincing enough to use one of the model's major feature in the forthcoming section, i.e., the distribution of the valence electrons is based on a hierarchy of what will be labelled recurrent localized states hereafter (HRLS). In these HRLSs, each state is defined by the given size of an atomic domain (basic PMIs or inflated PMIs at any inflation stage) and extends to all identical domains of the structure within local isomorphism. In each of these domains M/Nv^{3n} electrons/atoms are confined (time-averaged confinement) over distances scaling as Λv^n , in which M is the magic number, N the number of atoms in the basic units (PMIs here) of diameter Λ , v^3 is the inflation scale factor, and n , any integer, is the inflation order. Figure 4 shows two pieces of isomorphic subsets cut into the structure of an AlPdMn QC, corresponding to space extensions of two electronic eigenstates with, in each hatched area, M/N and M/Nv^3 electrons/atom respectively. It is now time to see how all this is acting on eigenstates and properties.

4. Eigenfunctions for HRLS and conductivity

In the introduction of the present paper, we explained that a plane wave with a wave vector \mathbf{k} couples with Fourier components of the structure whose Bragg vector \mathbf{G} is such that $|\mathbf{G}|/2^2 \leq |\mathbf{k}|$. This 'window' in reciprocal space defines the width of the 'state \mathbf{k} ' and the direct space extension is a subset of atomic sites resulting from a convolution of the whole structure by a repeated (recurrent) localization domain of size $2\pi/2|\mathbf{k}|$. Such a description is fully consistent with the HRLS introduced in the previous section. Recurrently localized states, or critical states, have eigenfunctions ψ_i over sites i . To differentiate these particular states from strictly localized or extended ones, one may ask the questions of on how many sites $n(\varepsilon)$ is $|\psi_i|^2$ larger than a small bound ε and how $n(\varepsilon)$ depends on the system size D . For truly extended states, ψ_i keeps the same value on all sites and $n(\varepsilon)_{ext} \approx D^3$; if a state is fully localized, it is not affected by the system growing around and $n(\varepsilon)_{loc} \approx D^0$ (constant value). Situations in between, with $n(\varepsilon)_{rec} \approx D^{3\beta}$ and $0 < \beta < 1$ may correspond

to recurrent localization. One may say that the $n(\varepsilon)_{rec}$ sites form a fractal subset of the structure with dimensionality $3\beta < 3$. It is reasonable to assume that this subset contains all domains of size d made equivalent by local isomorphism and defined by the geometry of the selfsimilar skeleton of the structure. Let us consider for instance a QC structure whose skeleton is based on a Mackay icosahedron geometry, with sites at the centre and on the 42 ‘surface’ positions being equivalent by local isomorphism; let us have also an inflation ratio v^3 for structure growth. After l inflation steps, the volume of each domain is $V \approx (v^9)^l = d^3$ and contains n_{rec} atomic positions such as $n_{rec} \approx d^{3\beta} \approx (43)^l$; it is trivial to calculate

$$\beta = \frac{\ln n_{rec}}{\ln V} - \frac{\ln 43}{9 \ln v} = 0.956$$

with $v = 1.548$ for AlPdMn QCs.

The eigenfunction $\psi(d)$ is attached to the structure subset made up of isomorphic areas of size d . Because of selfsimilarity of the structure, the eigenfunction $\psi(\chi d)$ for the structure subset made up of isomorphic areas of size χd is formally identical to $\psi(d)$ within attenuation to account for repartition over a larger number of atoms. Thus

$$|\psi(\chi d)|^2 = [1/n(\chi)]|\psi(d)|^2 \quad (6)$$

with $n(\chi)$ the scale factor that gives the number of atomic positions in a structure piece of size χd given that for size d . (6) is equivalent to

$$|\psi(d)| \approx 1/d^\alpha \quad \alpha = \frac{1}{2} \ln n(\chi) / \ln \chi. \quad (7)$$

Using again the same example with $\chi = v^3$ and $n(\chi) = 43$ gives

$$\alpha = \frac{1}{6} \ln 43 / \ln v = 3\beta/2 = 1.434. \quad (8)$$

Thus conductance decreases as $d^{-2.86}$ in this example, which precludes long-distance conductivity at 0 K for a perfect QC. Defects or/and atomic displacements may erase the potential barrier and restore transport occurrence. At this stage, it is important to realize that the exponents β and α , defining the power law dependence of the eigenfunctions and of their space extension, are in no way universal parameters. First of all they may vary from system to system, depending on the inflation scale factor or/and on the geometry of the cluster units. Moreover, α and β do not have single well defined values even for a given quasiperiodic structure; in (8), indeed, v does not suffer any ambiguity, but $n(\chi)$ fluctuates in the structure since local isomorphism does not state that nearest neighbours of given domains should be invariant. Then, the α and β numerical values as calculated above must be considered as no more than reasonable estimates in the remainder of the paper. In condensed matter, electrons in localized states can participate in conductivity via hopping between localization sites. For instance, the variable-range hopping model has been designed by Mott to express conductivity in disordered systems, with the idea that the hopping distance must increase as temperature is reduced to find localization sites with less distant energy levels. This leads to the famous $T^{-1/4}$ law:

$$\sigma = \sigma_0 \exp[-(T_0/T)^{1/4}]. \quad (9)$$

Such a variable-range hopping mechanism may apply to QC structures, with appropriate alteration. Let us consider the contribution $\sigma(d)$ to electron conductivity in a QC which arises from hopping in the recurrently localized state $\psi(d)$ that extends over the structure subset made up of isomorphic areas of size d . The jump frequency $s(d)$ from site to site of this subset is given by

$$s(d) = |\psi(d)|^2 \exp(-\Delta E/k_B T) \quad (10)$$

in which $\psi(d)$ is given by (7) and ΔE is the possible fluctuation of energy levels in all well-like potentials of size d , i.e. $\Delta E \approx d^{-2}$. Accordingly, (10) transforms into

$$\sigma(d) \approx s(d) \approx (1/d^{2\alpha}) \exp(-b/d^2 T) \quad (11)$$

in which b is a constant.

At high temperature the thermal activation term $\exp[-b/d^2 T]$ is close to its upper limit and the shortest hopping distance for the largest density of hopping electrons can be activated. Thus

$$\sigma_{ht} \approx \sigma(d_0) \approx (1/d_0^{2\alpha}) \exp\left[\frac{-b}{d_0^2 T}\right] \quad (12)$$

with d_0 of the order of 20 Å and $2\alpha = 2.9$ in the example already quoted.

At lower temperatures the exponential factor in (11) may become negligibly small unless larger hopping distances d are activated. At a given T value, the selected hopping distance d corresponds to a maximum of the jump frequency. Setting $\partial s(d)$ to zero gives $d^2(T) = b/\alpha T$ and

$$\sigma(T) \approx (\alpha/\beta)^\alpha \exp(-\alpha) T^\alpha \quad (13)$$

or $\sigma(T) \approx T^\alpha$ (with $\alpha = 1.43$ in the example of the AlPdMn QC).

Below a critical temperature (and beyond a critical distance d) the power law T^α may be lost experimentally because of extrinsic effects due to structure defects, boundaries, and the periodic approximant distortion which may restore the $T^{-1/4}$ law of the Mott model [52] or/and induce a \sqrt{T} contribution from Anderson weak localization. All in all, everything said in this section is reasonably well consistent with experimental results of electrical resistivity in QC systems such as AlPdRe, AlPdMn, or AlFeCu. By-products of the above calculation of the electrical conductivity concern the optical conductivity, the diamagnetic susceptibility, and the Hall coefficient. The optical conductivity $\sigma(\omega)$ does not follow at all the Drude behaviour expected from metallic systems and is very weak at all energies except around 1.12 eV, roughly where a broad resonance shows up. We have previously demonstrated that this is consistent with local oscillation of electrons between neighbour sites of a basic PMI recurrent state [28, 29]. The Hall coefficient R_H is in principle equal to the reciprocal number of the effective carriers; but this is strictly valid for free carriers only. With other transport mechanisms R_H remains roughly of the form $R_H \approx -1/\sigma(T)$, which gives

$$\begin{aligned} R_H &\approx -T^{-\alpha} \\ \frac{dR_H}{dT} &\approx \alpha T^{-(\alpha+1)} \end{aligned}$$

for QCs, using the expression of (13) for $\sigma(T)$. Negative values of R_H and positive temperature coefficient have indeed been observed experimentally [53] when the QC samples are of high structural and stoichiometric perfection.

In the model presented in this paper, the electronic density of states at the Fermi level is zero and valence electrons are distributed in saturated cluster levels (magic cluster at any length scale). The net spin on transition-metal atoms is then zero and Pauli paramagnetism does not show up, except at high temperature where the model may not apply any more.

Another transport phenomenon may also be described in a frame very similar to that of the HRLS scheme; this is thermal conductivity, where, in principle, both electronic and atomic vibrational states should participate. In the kinetic approximation thermal conductivity $\kappa(T)$ can be expressed as

$$\kappa(T) = \frac{1}{3} C(v) \Lambda \quad (14)$$

where C is a specific heat, $\langle v \rangle$ an average velocity for the thermal carriers, and Λ their mean free path. Heat can be transported by both electrons and phonons, if propagation does take place. At low temperature $\kappa(T)$, for both electric conductors and insulator crystals, is dominated by the phonon contribution up to temperatures around 20 K. Then this contribution vanishes drastically and $\kappa(T)$ becomes essentially zero at high temperature for insulators while keeping an almost constant value for conductors due to the electronic contribution (the Wiedman–Franz law).

In the description of QCs based on selfsimilar subsets of isomorphic domains, phonons or propagation of atomic vibrations must obey the same rules as introduced for electrons in the previous sections; vibrational states are attached to these subsets and communication between domains occurs via hopping. However, when the hopping distance exceeds some 100 Å the situation becomes similar to that of scattered phonons in crystal. This is actually the circumstances of the continuum approximation to which a Debye model applies. Thus, it can be said that in the limit of large wavelengths ($\lambda \geq 100$ Å) or small wave vectors ($|\mathbf{k}| \leq 0.06$ Å⁻¹) or else low-energy vibrational modes ($\hbar\omega \leq 1$ meV or about 10 K), pseudo-phonons exist in QCs and contribute to thermal conductivity. The density of states of these ‘propagating’ modes must be a power law ω^n of the energy, with n probably slightly larger than two because of the general trend of the energies to be pushed down by the umklapp-like effect mentioned previously. Thus, below about 10 K, one can calculate $\kappa(T)$ using (14) with C being a power law T^{n+1} at very low temperature and saturating in the Dulong–Petit regime around 10 K and above, $\langle v \rangle$ and Λ being essentially constant in this temperature range. This gives

$$\kappa(T)_{TBT} \approx T^{n+1} \quad n \geq 2$$

at very low temperature and turning into a plateau above 10 K. As already said, the electronic contribution to $\kappa(T)$ is negligibly small in this temperature range. To make an estimate, let us assume that each electron is able to carry the thermal energy $k_B T$; the number of carriers being proportional to the electrical conductivity $\sigma(T)$, one may write

$$\kappa(T)_{elec} \approx LT\sigma(T)$$

or

$$\kappa(T)_{elec} \approx LT^{\alpha+1}. \quad (15)$$

(15) is just an extension of the well known Wiedman–Franz law. The coefficient L cannot exceed the Lorentz free electron value $\pi^2 k_B^2 / 3e^2$, which maintains the $\kappa(T)_{elec}$ contribution to thermal conductivity well below 1% up to $T \approx 100$ K, for QCs of the systems AlPdMn, AlPdRe and AlFeCu.

Above $T = 10$ K and up to about 100 K the thermal conductivity $\kappa(T)$ indeed maintains a constant value [54]. The further increase which is observed above 100 K [54] may originate from the electronic contribution, following the law shown in (15), but we cannot *a priori* eliminate possible contribution from phonon-assisted hopping of the recurrently localized vibration modes corresponding to each class of isomorphic clusters. Let us call these modes ‘clustrons’ for brevity. They are conceptually very similar to fractons [55]. For this purpose, (14) may be conveniently rewritten as

$$\kappa(T)_{clustron} = \frac{1}{3} C \Lambda^2 \tau_\Lambda^{-1} \quad (16)$$

in which Λ is now the average distance between isomorphic sites and is also the average jump length with the frequency τ_Λ^{-1} . Mathematical derivations similar to those having

produced (13) allow us to relate Λ and τ_{Λ}^{-1} to temperature, so

$$\Lambda = (\beta/\alpha k_B T)^{1/2} \quad \tau_{\Lambda}^{-1} \approx (\alpha k_B/\beta)^{\alpha} \exp(-\alpha) T^{\alpha}. \quad (17)$$

Assisted hopping of clustrons is a conduction mechanism that is very close to tunnelling and the corresponding excitation should contribute to the specific heat with linear temperature dependence $C = \gamma T$ at low temperature and C becoming constant as T increases.

Substituting (17) into (16) thus gives

$$\kappa(T)_{clustron} \approx T^{\alpha-1}. \quad (18)$$

Combining (15) and (18) gives the temperature behaviour of the thermal conductivity of QCs above 100 K:

$$\kappa(T) = AT^{\alpha-1} + BT^{\alpha+1}.$$

At the highest temperature, $\kappa(T)$ is mainly influenced by the $T^{\alpha+1}$ electronic term (the $T^{2.43}$ law for AlPdMn) which is again close to observations [54].

5. Discussion and conclusion

In the present paper we have tried to bring insight into the nature and the particular behaviour of electronic (and also vibrational) eigenstates in QCs. The basic idea reported on here is that eigenmodes follow the selfsimilar features of the structure and are assigned to extend over site subsets gathering locally isomorphic domains. These isomorphic domains correspond, for each eigenstate, to a given inflated version of basic atomic units. These basic atomic units are very stable ‘magic’ clusters whose geometry and composition are strictly defined within selfconsistency rules dominated by selfsimilarity. Most of the electromagnetic or thermal properties of QCs can be reasonably understood within such a scheme.

Most of the bonding electrons being essentially trapped into cluster levels, with exchanges limited to intraband-like mechanisms, also suggests that QCs must be poorly reactive to any external action. They have actually a very low mechanical response, they resist corrosion and their surfaces are weakly adhesive, refuse easy wetting, and exhibit incredibly small friction coefficients. The effectiveness and impact of the rigid clusters on mechanical properties is especially spectacular, with an extremely brittle behaviour up to about 100 K prior melting. The rigid clusters prevent easy simple gliding and these clusters cannot be cut or deformed without destabilization of the structure. Cracks have been observed to propagate in between the clusters [56]. The surface morphology upon fracture test shows the features typical of solids with strong anisotropic atomic bonds and in which atomic transport, if any, is only very slow.

Finally the magic cluster scheme may also shed some doubts on a true quasiperiodic structure of the QC surfaces. In any case, these surfaces when in their natural state will be very rough due to emerging rigid clusters. This has been actually observed on cleaved samples [32]. On the other hand, surface reconstruction, when allowed, can occur only if at least a ‘layer’ of clusters is destroyed and rearranged; the corresponding abrupt cut of the structure by a surface must also account for relaxation of the selfsimilarity rules dominating the bulk. Chemical compositions as measured on reconstructed QC surfaces [57, 58] of single grains of AlPdMn shows a net depletion in Mn, which suggests that a layer of the ξ approximant [51] may form at surfaces, with perhaps some sort of a structural gradient profile to reach the icosahedral geometry down in the bulk. Considering this point may be an interesting challenge for further investigations.

References

- [1] Janot C 1994 *Quasicrystals: a Primer* 2nd edn (Cambridge: Cambridge University Press)
- Janot C 1991 *Quasicrystals, the State of the Art* ed D P Di Vincenzo and P J Steinhart (Singapore: World Scientific)
- Janot C 1990 *Quasicrystals* ed T Fujiwara and T Ogawa (Berlin: Springer)
- Janot C 1995 *Proc. 5th Int. Conf. on Quasicrystals (Avignon, France, 1995)* ed C Janot and R Mosseri (Singapore: World Scientific)
- [2] Cornier-Quiquandon M, Quivy M, Lefebvre S, Elkaim E, Heger G, Katz A and Gratiat D 1991 *Phys. Rev. B* **44** 2071
- [3] Boudard M, de Boissieu M, Janot C, Heger G, Beeli C, Nissen H U, Vincent H, Ibberson R, Audier A and Dubois J M 1992 *J. Phys.: Condens. Matter* **4** 10 149
- [4] Pierce F S, Poon S J and Guo Q 1993 *Science* **261** 737
- [5] Chernikov M A, Bianchi A and Ott R H 1995 *Phys. Rev. B* **51** 153
- [6] De Giorgi L, Chernikov M A, Beeli C and Ott H R 1993 *Solid State Commun.* **87** 721
- [7] Dubois J M, Kang S S and Perrot A 1994 *Mater. Sci. Eng. A* **179/180** 122
- [8] Akiyama H, Honda Y, Hashimoto T, Edagawa K and Takeuchi A 1993 *Japan. J. Appl. Phys. B* **7** L1003
- Honda Y, Edagawa K, Yoshika A, Hashimoto T and Takeuchi S 1994 *Japan. J. Appl. Phys. A* **9** 4929
- [9] Poon S J 1992 *Adv. Phys.* **41** 303
- [10] Berger C, Grenet T, Lindqvist P, Lanco P, Grieco J C, Fourcaudot G and Cyrot-Lackmann F 1993 *Solid State Commun.* **87** 977
- [11] Pierce F S, Guo Q and Poon S J 1994 *Phys. Rev. Lett.* **73** 2220
- [12] Perrot A and Dubois J M 1995 *Quasicrystals* ed C Janot and R Mosseri (Singapore: World Scientific) p 586
- [13] Feuerbacher M, Baufeld B, Rosenfeld R, Bartsch M, Hanke G, Beyss M, Wollengarten M, Messerschmitt U and Urban K 1995 *Phil. Mag. Lett.* **71** 91
- [14] Janot C 1996 *Europhys. News* **27** 60
- [15] Poussiguet G, Benoît C, Azougarh A, de Boissieu M and Currat R 1994 *J. Phys.: Condens. Matter* **6** 659
- [16] Windish M, Hafner J, Krajci M and Mihalkovic M 1994 *Phys. Rev. B* **49** 8701
- Krajci M, Windish M, Hafner J and Kress G 1995 *Phys. Rev. B* **51** 17 355
- [17] Simon H, Baake M and Kramer P 1995 *Z. Phys. B* **98** 509
- [18] Fujimara T, Mitsui T and Yamamoto S 1996 *Phys. Rev. B* **53** R2910
- [19] Mayou D, Berger C, Cyrot-Lackmann F, Klein T and Lanco P 1993 *Phys. Rev. Lett.* **70** 3915
- [20] Krajci M, Windish M and Hafner J 1995 *Phys. Rev. B* **51** 17 355
- [21] Trambly de Laissardière G and Mayou D *Phys. Rev. Lett.* submitted
- [22] Trambly de Laissardière G, Roche S and Mayou D *Mater. Sci. Eng. A* at press
- [23] Onada G Y, Steinhardt P J, Di Vincenzo D P and Socolar J E S 1988 *Phys. Rev. Lett.* **60** 2653
- [24] Jeong H C and Steinhardt P J 1994 *Phys. Rev. Lett.* **73** 1943
- [25] Quemerais P 1994 *J. Physique I* **4** 1669
- [26] Dzugutov M 1992 *Phys. Rev. A* **46** R2984
- Dzugutov M 1993 *Phys. Rev. Lett.* **70** 2924
- [27] Janot C and de Boissieu M 1994 *Phys. Rev. Lett.* **72** 1674
- [28] Janot C 1996 *Phys. Rev. B* **53** 181
- [29] Janot C and Dubois J M 1996 *Les Quasicristaux: Matière à Paradoxes* (Paris: Editions de Physique) at press
- [30] Zurkirsh M, Atrei A, Erbudak M and Hochstrasser M 1996 *Phil. Mag. Lett.* **73** 107
- [31] Naumovic D private communication
- [32] Ebert P, Feuerbacher M, Tamura N, Wollengarten M and Urban K 1996 *Phys. Rev. Lett.* at press
- [33] Guo B C, Kerns K P and Castleman A W Jr 1992 *Science* **255** 1411
- [34] Knight W D, Clemenger K, de Heer W A, Saunders W A, Chou M Y and Cohen M L 1984 *Phys. Rev. Lett.* **52** 2141
- [35] Leuchtner R E, Harms A C and Castleman A W Jr 1989 *J. Chem. Phys.* **91** 2753
- [36] Khanna S N and Jena P 1992 *Phys. Rev. Lett.* **69** 1664
- Khanna S N and Jena P 1993 *Phys. Rev. Lett.* **71** 208
- [37] Khanna S N and Jena P 1994 *Chem. Phys. Lett.* **218** 383
- Khanna S N and Jena P 1994 *Chem. Phys. Lett.* **219** 479
- [38] Khanna S N and Jena P 1995 *Phys. Rev. B* **51** 13 705
- [39] Wu X, Kycia S W, Olson C G, Benning P J, Goldman A I and Lynch D W 1995 *Phys. Rev. Lett.* **75** 4540
- [40] Zurkirsh M, Atrei A, Hochstrasser M, Erbudak M and Kortan A R 1996 *J. Electron Spectrosc. Relat. Phenom.* **77** 233

- [41] Tsai A P, Inoue A and Masumoto T 1990 *Phil. Mag. Lett.* **62** 95
- [42] Kycia S W, Goldman A I, Lograsso T A, Delancy D W, Sutton M, Dufresne E, Brüning R and Rodricks B 1993 *Phys. Rev. B* **48** 3544
- [43] de Boissieu M, Durand-Charre M, Bastie P, Carabelli A, Boudard M, Bessiere M, Lefebvre S, Janot C and Audier A 1992 *Phil. Mag. Lett.* **65** 147
- [44] Boudard M, Bourgeat-Lami E, de Boissieu M, Janot C, Durand-Charre M, Klein H, Audier M and Hennion B 1995 *Phil. Mag. Lett.* **71** 11
- [45] Janot C 1996 *Proc. Int. Symp. on the Science and Technology of Atomically Engineered Materials* ed P Jena, S N Khanna and B K Rao (Singapore: World Scientific) p 221
- [46] Belin E, Dankhazi Z, Sadoc A and Dubois J M 1994 *J. Phys.: Condens. Matter* **6** 8771
Belin E, Dankhazi Z, Sadoc A and Dubois J M 1994 *Eur. Phys. Lett.* **26** 677
- [47] Basov D N, Timusk T, Barakat F, Greedan J and Grushkjo B 1994 *Phys. Rev. Lett.* **72** 1937
Basov D N, Poon S J and Timusk T 1995 *Preprint*
- [48] Parker L J, Atou T and Badding J V 1996 *Science* **273** 95
- [49] Urban K, Wollengarten M and Wittmann R 1993 *Phys. Scr. T* **49** 360
- [50] de Boissieu M, Boudard M, Hennion B, Bellissent R, Kycia S, Goldman A I, Janot C and Audier M 1995 *Phys. Rev. Lett.* **75** 89
Boudard M, de Boissieu M, Letoublon A, Hennion B, Bellissent R and Janot C 1996 *Europhys. Lett.* **33** 199
- [51] Audier M, Durand-Charre M and de Boissieu M 1993 *Phil. Mag. Lett. B* **68** 607
- [52] Guo Q and Poon S J 1996 *Phys. Rev. Lett.* at press
- [53] Berger C, Gignoux C, Tjernberg O, Lindqvist P, Cyrot-Lackmann F and Calvayrac Y 1995 *Physica B* **203** 44
- [54] Dubois J M and Perrot A 1993 *Ann. Chim.* **18** 501
- [55] Nakayama T, Yakubo K and Orbach R L 1994 *Rev. Mod. Phys.* **66** 1
- [56] Krul F, Mikulla R, Gumbsch P and Trebin H R 1996 to be published
- [57] Schaub T M, Bürgler D E, Güntherodt H J, Suck J B and Audier M 1995 *Appl. Phys. A* **61** 491
- [58] Chang S L, Anderegg J W and Thiel P A 1996 *J. Non-Cryst. Solids* **195** 95
Chang S L, Chin W B, Zhang C M, Jenks C J and Thiel P A 1995 *Surf. Sci.* **337** 135